Journal of Non-Crystalline Solids 356 (2010) 2641–2644

Correlation of network structure with devitrification mechanism in lithium and sodium diborate glasses

B. Chen [a], U. Werner-Zwanziger [a], J.W. Zwanziger [a,*], M.L.F. Nascimento [b], L. Ghussn [b], E.D. Zanotto [b]

[a] Dept. of Chemistry and Institute for Research in Materials, Dalhousie University, Halifax, NS B3H 4J3 Canada
[b] Departamento de Engenharia de Materiais, Universidade Federal de São Carlos, 13565-905 São Carlos, SP, Brazil

ARTICLE INFO

Article history:
Received 7 October 2009
Available online 24 August 2010

Keywords:
Glass devitrification;
Homogeneous nucleation and growth;
Heterogeneous nucleation and growth;
Nuclear magnetic resonance

ABSTRACT

The intermediate-range structure of the network former in lithium and sodium diborate was studied using nuclear magnetic resonance spectroscopy. Specifically, $^{11}B\{^{10}B\}$ rotational-echo double resonance experiments were employed to determine the distribution of dipole couplings between these isotopes and in this way determine whether the intermediate range order of the borate network was the same in the glasses as in the crystal forms of these compounds. It was found that in the lithium diborate case the networks are in fact similar between glass and crystal, while in sodium diborate they differ substantially. Because lithium diborate shows homogeneous nucleation and growth on the laboratory time scale while sodium diborate does not, it was concluded that structural similarity between glass and crystal of the glass former correlates strongly with nucleation mechanism.

1. Introduction

Glass devitrification proceeds by one of two classical mechanisms, namely heterogeneous nucleation and growth triggered by impurities or surfaces, or by homogeneous nucleation and growth throughout the sample volume [1,2]. While any non-equilibrium liquid or glass should undergo homogeneous nucleation if given clean enough conditions and enough time, here we distinguish between systems which undergo homogeneous nucleation on typical laboratory time scales and those that do not. Under such restrictions there are a number of well-studied examples, of rather simple chemistry, which devitrify typically by one process or the other, and it is of interest to understand why one type of behavior is observed in some systems and the other type in others.

In particular we consider the possibility that the similarity between the glass and crystal structure ultimately formed is the significant indicator for which type of mechanism will be followed [3,4]. To focus the discussion further we consider systems which crystallize congruently, that is to crystals with the same chemical composition as the original liquid and glass. Then, the hypothesis can be rephrased that the glass and crystal must have similar structures in order to exhibit homogeneous nucleation and growth on the laboratory time scale, and otherwise will show heterogeneous nucleation and growth. Here by structure we have in mind both local and intermediate range order [5], although we anticipate that intermediate range order will be more diagnostic. Generally the short-range order of glass and an isochemical crystal are very similar [6], because the bonding electron configurations are essentially the same. At longer length scales, however, there can be significant differences.

This hypothesis has been considered in several earlier studies. In metallic systems, the correlation between structural mismatch of the liquid and solid on the one hand and nucleation on the other, is termed Frank's Hypothesis and was confirmed experimentally by Kelton and colleagues [7]. In inorganic glasses the correlation was found for the local structure around metallic cations [4]. Concerning the glass former in inorganic systems, Schneider et al. [3] considered the distribution of Q species in various silicates, and observed a correlation between the distribution of Q species in the glass and crystal phases of several systems. Deubener [8] showed that intermediate range order increases in supercooled liquids as they are cooled, and suggested that this order provides nucleation sites for volume nucleation in deeply undercooled melts. However, whether this ordering is similar to that found in the crystals that ultimately form was not explored.

Previously we studied in detail the cation distributions in lithium and sodium disilicate ($Li_2O{\cdot}2SiO_2$ and $Na_2O{\cdot}2SiO_2$, ref. [9]) and in lithium and sodium diborate ($Li_2O{\cdot}2B_2O_3$ and $Na_2O{\cdot}2B_2O_3$, submitted for publication). In these studies we compared both cation-cation and cation-glass-former (silicon or boron) distance distributions between the glass and the final crystal phases. In both cases we found that the glass structure and the crystal structure of the lithium compounds were quite similar, and both cases show homogeneous nucleation and growth on the laboratory time scale. In contrast, both sodium compounds showed marked differences between the glass and crystal structures, and both also show only heterogeneous nucleation and growth on typical laboratory time scales. For the sodium compounds,

* Corresponding author. Tel.: +1 902 494 1960; fax: +1 902 494 1867.
E-mail address: jzwanzig@dal.ca (J.W. Zwanziger).

0022-3093/$ – see front matter © 2010 Elsevier B.V. All rights reserved.
doi:10.1016/j.jnoncrysol.2010.04.053

the crystals formed (various phases of $Na_2Si_2O_5$ and $Na_2B_4O_7$, respectively) show layered structures [10–13], while the glasses show nuclear magnetic resonance (NMR) signatures indicative of more homogeneous distributions of the various species. These studies support the hypothesis that similar structures correlate with homogeneous nucleation and growth while dissimilar structures favor the heterogeneous mechanism.

However, because of the significant difference in time scales between cation and glass-former motion at temperatures near the glass transition [14], it is questionable whether the cation distributions themselves, even including the cation-glass-former distance distributions, are sufficient to test the hypothesis. It could be that fast cation motion during the nucleation event destroys any real correlation between structural similarity of the quenched glass and the crystal, making the previously report results at best coincidental. Therefore we undertook to study the distance distributions within the glass-former itself. In the present contribution we report NMR measurements of the boron–boron distance distributions in lithium diborate and sodium diborate glass, and compare these results to the crystal structures. We find again significant differences between the glass and crystal structure in the sodium diborate case, while in the lithium diborates these distributions are almost the same. Thus even focusing only on the glass former, it appears that similar structures in glass and crystal are necessary for homogeneous nucleation and growth to be observable on the laboratory time scale.

2. Experimental methods

2.1. Sample preparation

The $Li_2O{\cdot}2B_2O_3$ (L2B) and $Na_2O{\cdot}2B_2O_3$ (N2B) samples were prepared by the standard melt-quenching approach. A typical procedure was the following (see Table 1): mixtures of starting materials (alkali diborate decahydrates of analytical purity) in appropriate proportions were melted in platinum crucibles in a furnace up to 900–1000 °C (T_m) for 2–3 h (t_m) before quenching in air.

The splat cooling method with iron molds was applied for N2B glass, and L2B glass was obtained by quenching the platinum crucible with supercooled liquid inside. Part of the glass samples were crystallized by holding them at specific temperatures T_c for sufficient times t_c. In order to reduce the T_1 relaxation time of the observed nuclei, trace amounts of paramagnetic Mn^{2+} were added, which is regarded not to affect the structure of the glass [15].

2.2. Phase identification and thermal analysis

Powder X-ray diffraction measurements were conducted to determine the phase purity of the crystal samples. The patterns were recorded on a Bruker D8 Advance powder X-ray diffractometer in Bragg–Brentano configuration using Cu $K\alpha$ radiation (wavelength 1.5406 Å) and a graphite monochromator with 0.02°/s step width. Differential scanning calorimetry (DSC) analysis by means of a Netzsch 404 apparatus was done using finely powdered samples under heating rate of 10 °C/min. The various temperatures, including glass transition (T_g), onset (T_x) and the maximum peak (T_p) of the crystallization as well as the liquidus (T_L) temperatures were obtained from the resulting curves (Table 1).

2.3. NMR studies

All the NMR experiments were carried out with a 3.2-mm Bruker MAS probe on a Bruker Avance NMR spectrometer equipped with three radiofrequency (rf) channels operating at a magnetic field of 16.4 T. The Larmor frequencies of ^{10}B and ^{11}B were 75.24 and 224.67 MHz, respectively. All the spectra were referenced to solid $NaBH_4$ at −42.16 ppm. For the ^{10}B MAS spectra, single pulse acquisition was applied with a short RF pulse (rf field strength of 125 kHz) of 0.2 μs. The spinning rate was 10 kHz and the recycle delay was 30 s. For the rotational echo double resonance (REDOR) experiments [16,17], the pulse lengths for the observed nucleus ^{11}B were optimized by maximizing the signal from the experiments without applying pulses to the coupled nucleus ^{10}B, resulting in $\pi/2$ and π pulses of 3.25 μs and 7 μs respectively. The π pulse on the unobserved nucleus was optimized by minimizing the signal of the experiment with ^{10}B dephasing, leading to π pulses of 13.5 μs for a power of 18.5 kHz. In most experiments 8 or 16 scans were used to obtain better average results. The spinning speed was 10 kHz with typical recycle delays of 40 to 60 seconds.

3. Results and discussion

The short range order of the network former (borate) in L2B and N2B has already been discussed, based on ^{11}B MAS and multiple quantum MAS NMR experiments (Chen et al., submitted). Essentially, in the glasses three and four coordinate boron are observed (B3 and B4, respectively), in ratios closely matching those in the corresponding crystal phases [13,18]. In L2B, the B3 site in the glass is very much like that in the corresponding crystal. In crystalline N2B there are 5 distinct B3 sites, with similar quadrupole couplings but a range of quadrupole asymmetries. In the glass, only the sites with intermediate asymmetry are observed, not the two sites with respectively very small and very large asymmetry. Other than this minor difference, however, the short range order of the borate glass former in L2B and N2B is quite similar in the glass and crystal phases.

Fig. 1 shows the ^{10}B MAS spectra for the various samples. In all cases only a single resonance is observed. This can be understood by realizing that ^{10}B, being spin-3, has no analog to the central transition observed in ^{11}B and other half-integral spin nuclei [19]. Its spectrum is thus broadened by first-order quadrupole effects. Taking into account the larger electric quadrupole moment of ^{10}B as compared to ^{11}B (8.459 fm^2 versus 4.059 fm^2 [20]), the quadrupole coupling is 5.5 MHz for the B3 sites. This broadening in the first-order spectra renders the B3 sites essentially unobservable, and hence only the B4 sites are excited and detected. This observation is important below as we discuss the REDOR experiments.

The $^{11}B\{^{10}B\}$ REDOR experiment is similar to other heteronuclear REDOR experiments, even though the nuclei involved are chemically identical. Because the two species have different gyromagnetic ratios, they behave exactly as any other heteronuclear pair. The REDOR data is acquired as pairs of spectra, one without refocusing of the partner spin, and one with. The spectra are termed S_0 and S_1, and in this case

Table 1
Preparation conditions for lithium diborate (L2B) and sodium diborate (N2B) used in this work, and results of thermal analysis. The crystallized form of L2B and both glass and crystal forms of N2B were doped with 0.05% MnO_2 in order to decrease relaxation times in the NMR experiments.

Initial	Glass melting		Crystallization		Thermal analysis			
	T_m/°C	t_m/h	T_c/°C	t_c/h	T_g/°C	T_X/°C	T_p/°C	T_L/°C
$Li_2B_4O_7{\cdot}10H_2O$	1000	2	510	20	490	530	552	920
$Na_2B_4O_7{\cdot}10H_2O$	900	3	520	3	457	540	552	746

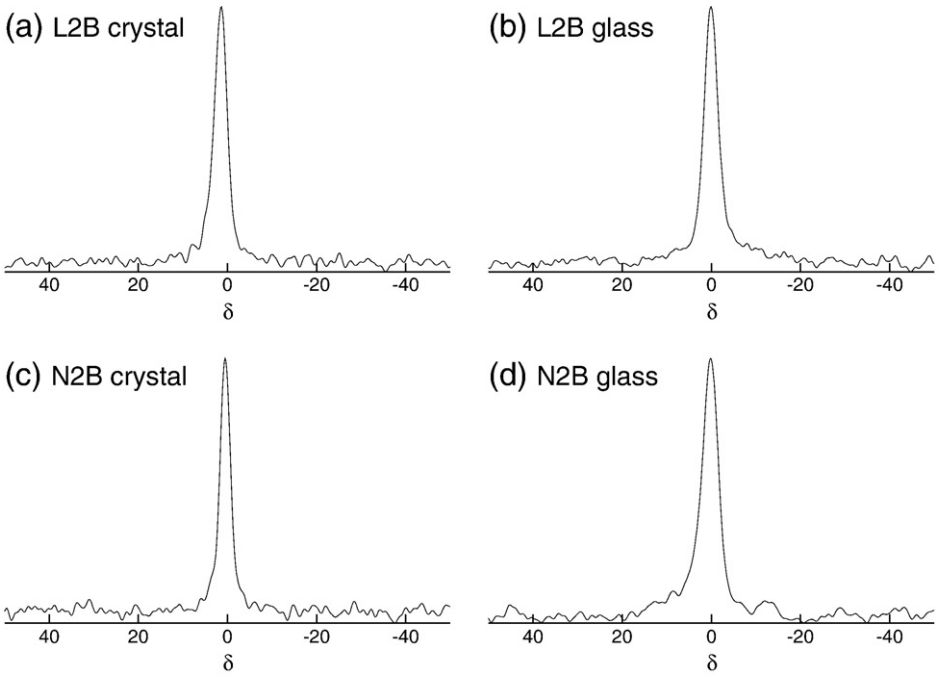

Fig. 1. ^{10}B MAS NMR spectra.

the observed spin is ^{11}B and the partner spin is ^{10}B. The spectra are measured as a function of refocusing time NT_r, where T_r is the rotor period of the spinning sample. The initial part of the REDOR dephasing curve can be fit to

$$\frac{S_0 - S_1}{S_0} = (NT_r)^2 f M_2, \quad (1)$$

where f is a calibration factor that takes into account imperfect bandwidth excitation and other experimental factors, and M_2 is the second moment of the distribution of dipole couplings for the investigated spin pair [21]. The factor M_2 itself is related to structure as follows [21,22]:

$$M_2 = \frac{4}{15}\left(\frac{\mu_0}{4\pi}\right)^2 \hbar^2 \gamma_S^2 \gamma_I^2 S(S+1) \sum r_{IS}^{-6}, \quad (2)$$

for observed spin I and dephased spin S, where μ_0 is the vacuum permeability, γ the gyromagnetic ratio, and r the internuclear distance. Put simply, fast dephasing implies a large M_2 and hence close spins, while slow dephasing implies a small M_2 and distant spins. Because of the calibration factor in Eq. (1) and the complicated dependence on distances in Eq. (2), this experiment is well-suited for assessing structural differences between two samples but not so reliable for measuring specific distances between quadrupolar nuclei [5].

The second moment values derived from the REDOR experiments are summarized in Table 2, and the REDOR difference data and fits are shown in Fig. 2. Because of the first-order broadening in the ^{10}B spectra, the REDOR curves give essentially information about correlations between all boron sites, from the ^{11}B excitation and detection, and B4 sites, from the ^{10}B dephasing. While the B3 and B4

Table 2
Calculated and measured second moments of the dipole distributions for the correlations between all boron sites and four-fold-coordinate boron sites, as deduced from ^{11}B{^{10}B} REDOR experiments.

Sample		$M_{2,calc}/10^6$rad^2/sec^2	scaled M2,expt/10^6rad^2/s^2
L2B	Crystal	2.35	2.35
	Glass		2.5 ± 0.3
N2B	Crystal	1.63	1.63
	Glass		4.0 ± 0.4

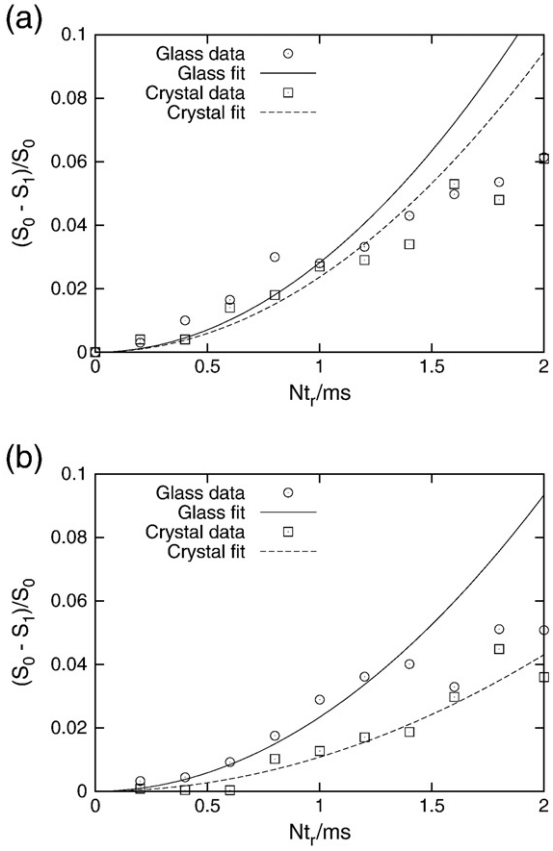

Fig. 2. REDOR difference curves and fits for (a) lithium diborate crystal and glass, and (b) sodium diborate crystal and glass.

sites are well-resolved in ^{11}B spectra, we saw no difference in dephasing of these two sites that was clearly above the noise threshold. Therefore we interpret the dephasing in terms distances between all boron sites and B4 sites.

The M_2 values reported in Table 2 were determined as follows. First, from the crystal structures, the distances from B3 sites to B4 sites and from B4 sites to B4 sites were summed over a 50 Å range, which gave convergence of the $\sum r^{-6}$ factor to better than one part in 10^6. These two sums were then combined with weights reflecting the population of B3 and B4 sites in each crystal (1/2 and 1/2 in L2B, 5/8 and 3/8 in N2B), and multiplied by the physical constants in Eq. (2) to obtain a combined M_2. This value was then multiplied by the natural abundance of ^{10}B to get the effective M_2 for the crystal. Then, to set the calibration factor in Eq. (1), the M_2 extracted from a fit to the data for the crystal was scaled such that it agreed with the calculated value. Finally, the M_2 extracted from a fit to the glass data was scaled by the same factor. Because of the close similarity of the local structure between the glass and crystal, the excitation and detection efficiencies should be the same in both samples, thus this procedure for setting the calibration factor is sufficient for comparing the glass sample with the crystal sample. A consistency check of the data arises from noting that for the two crystals, $M_2(\mathrm{L2B})/M_2(\mathrm{N2B}) = 2.35/1.63 = 1.44$. Therefore the data for the crystals should show a ratio of REDOR signals at equal times of 1.44, and comparing the data at two rotor cycles (see Fig. 2) gives a signal ratio of about $0.06/0.04 = 1.5$, in reasonable agreement with the prediction.

At the qualitative level, the difference in boron REDOR between L2B and N2B is clear. In L2B, the glass and crystal samples show essentially the same dephasing rate. Specifically this means that typical distances between boron and B4 sites are the same in the glass and the crystal, consistent with our earlier finding that the lithium–boron and lithium–lithium distances are similar in both forms. In N2B, however, we observe that the glass sample shows significantly faster dephasing, indicating that boron–boron distances are somewhat shorter than in the crystal. The likely structural interpretation of this observation is that the glass has a more homogeneous three-dimensional structure, unlike the crystal, which is layered [13]. Therefore in the glass, on average the borons are closer to each other than in the crystals, where the boron oxide layers are separated by the sodium cations. Consistent with this view is the fact that we found previously that the sodium–sodium distances are increased in the glass and the sodium–boron distances are decreased, again as the layers are broken up to form the glass. Finally, we note that, regardless of interpretation, the data show that the L2B glass and crystal have similar length scales for glass former (borate) ordering, while N2B glass and crystal differ significantly.

4. Conclusions

In this work we showed that the glass former structure correlated with nucleation mechanism. Lithium diborate, which on the laboratory time scale devitrifies by homogeneous nucleation and growth, shows essentially the same ordering length scale between the glass and the crystal. Sodium diborate, which devitrifies by the heterogeneous mechanism, shows a substantial difference in ordering scale between glass and crystal. Therefore, not only in terms of cation order, as we showed earlier, but also in terms of glass former order, is there a strong correlation between structure and devitrification mechanism.

Acknowledgments

Funding from the Inter-American Materials Collaboration program of NSERC and the instrumental support from IRM (Dalhousie University) are acknowledged. This work was also financially supported by the Brazilian research funding agency FAPESP (Processes 2004/10703-0 and 2007/08179-9). We also thank Anita Lam (Chemistry Department, University of British Columbia) for the XRD measurement, and phase identification.

References

[1] W. Höland, G.H. Beall, Glass-Ceramic Technology, American Ceramics Society, Westerville, USA, 2002.
[2] L.A. Souza, M.L.G. Leite, E.D. Zanotto, M.O. Prado, Crystallization statistics. A new tool to evaluate glass homogeneity, J. Non-Cryst. Solids 351 (2005) 3579–3586.
[3] J. Schneider, V.R. Mastelaro, H. Panepucci, E.D. Zanotto, ^{29}Si MAS-NMR studies of Q_n structural units in metasilicate glasses and their nucleating ability, J. Non-Cryst. Solids 273 (2000) 8–18.
[4] V.R. Mastelaro, E.D. Zanotto, N. Lequeux, R. Cortès, Relationship between short-range order and ease of nucleation in $Na_2Ca_2Si_3O_9$, $CaSiO_3$ and $PbSiO_3$ glasses, J. Non-Cryst. Solids 262 (2000) 191–199.
[5] H. Eckert, S. Elbers, J.D. Epping, M. Janssen, M. Kalwei, W. Strojek, U. Voigt, Dipolar solid state NMR approaches towards medium-range structure in oxide glasses, Topics in Current Chemistry: New Techniques in Solid State NMR, vol. 246, Springer, Berlin, 2005, pp. 195–233.
[6] P.H. Gaskell, Medium-range structure in glasses and low-Q structure in neutron and X-ray scattering data, J. Non-Cryst. Solids 351 (2005) 1003–1013.
[7] K.F. Kelton, G.W. Lee, A.K. Gangopadhyay, R.W. Hyers, T.J. Rathz, J.R. Rogers, M.B. Robinson, D.S. Robinson, First X-ray scattering studies on electrostatically levitated metallic liquids: demonstrated influence of local icosahedral order on the nucleation barrier, Phys. Rev. Lett. 90 (2003) 195504.
[8] J. Deubener, Structural aspects of volume nucleation in silicate glasses, J. Non-Cryst. Solids 351 (2005) 1500–1511.
[9] J.G. Longstaffe, U. Werner-Zwanziger, J.F. Schneider, M.L.F. Nascimento, E.D. Zanotto, J.W. Zwanziger, Intermediate-range order of alkali disilicate glasses and its relation to devitrification mechanism, J. Phys. Chem. C 112 (2008) 6151–6159.
[10] J. Williamson, F.P. Glasser, The crystallization of $Na_2O{\cdot}2SiO_2$–SiO_2 glasses, Phys. Chem. Glasses 7 (1966) 127–138.
[11] A.K. Pant, D.W.J. Cruickshank, The crystal structure of α-$Na_2Si_2O_5$, Acta Cryst. B 24 (1968) 13–19.
[12] A.K. Pant, A reconsideration of the crystal structure of β-$Na_2Si_2O_5$, Acta Cryst. B 24 (1968) 1077–1083.
[13] J. Krogh-Moe, The crystal structure of sodium diborate, $Na_2O(B_2O_3)_2$, Acta Cryst. B 30 (1974) 578–582.
[14] C.A. Angell, Dynamic processes in ionic glasses, Chem. Rev. 90 (1990) 523.
[15] M.G. Mortuza, R. Dupree, D. Holland, Studies of the effect of paramagnetic impurity in the structure of sodium disilicate glass, J. Mater. Sci. 35 (2000) 2829–2832.
[16] T. Gullion, J. Schaefer, Rotational-echo double-resonance NMR, J. Magn. Reson. 81 (1989) 196–200.
[17] Y. Pan, T. Gullion, J. Schaefer, Determination of C–N internuclear distances by rotational-echo double-resonance NMR of solids, J. Magn. Reson. 90 (1990) 330–340.
[18] J. Krogh-Moe, Refinement of the crystal structure of lithium diborate, $Li_2O(B_2O_3)_2$, Acta Cryst. B 24 (1968) 179–181.
[19] B.F. Chmelka, J.W. Zwanziger, Solid-state NMR Line Narrowing Methods for Quadrupolar Nuclei: Double Rotation and Dynamic-Angle Spinning, in: B. Blümich, R. Kosfeld (Eds.), Solid State NMR IV, Vol. 33 of NMR Basic Principles and Progress, Springer, Berlin, 1994, pp. 79–124.
[20] P. Pyykkö, Year-2008 nuclear quadrupole moments, Mol. Phys. 106 (2008) 1965–1974.
[21] M. Bertmer, L. Züchner, J.C.C. Chan, H. Eckert, Short and medium range order in sodium aluminoborate glasses. 2. Site connectivities and cation distributions studied by rotational echo double resonance NMR spectroscopy, J. Phys. Chem. B 104 (2000) 6541–6553.
[22] J.H. Van Vleck, The dipolar broadening of magnetic resonance lines in crystals, Phys. Rev. 74 (9) (1948) 1168–1183.